



# Electrochromic biosensors based on screen-printed Prussian Blue electrodes

Miguel Aller-Pellitero<sup>a</sup>, Joséphine Freneau<sup>b</sup>, Rosa Villa<sup>a,c</sup>, Gonzalo Guirado<sup>d</sup>, Boris Lakard<sup>b</sup>, Jean-Yves Hihn<sup>b</sup>, F. Javier del Campo<sup>a,\*</sup>

<sup>a</sup> Instituto de Microelectrónica de Barcelona, IMB-CNM (CSIC), Esfera UAB, Campus Universidad Autónoma de Barcelona, 08193, Bellaterra, Barcelona, Spain

<sup>b</sup> Institut UTINAM, UMR 6214 CNRS/Univ. Bourgogne Franche-Comté, 16 route de Gray, 25030, Besançon, France

<sup>c</sup> CIBER-BBN, Networking Centre on Bioengineering, Biomaterials and Nanomedicine, Barcelona, Spain

<sup>d</sup> Departament de Química, Universitat Autònoma de Barcelona, Facultat de Ciències, 08193, Cerdanyola del Vallès, Spain

## ARTICLE INFO

### Keywords:

Prussian Blue electrodes  
Screen-printed electrodes  
Spectroelectrochemistry  
Biosensors  
Hydrogen peroxide detection  
Glucose sensing

## ABSTRACT

Prussian Blue (PB)-modified graphite screen-printed electrodes are increasingly being used in electrochemical biosensors. However, they do not allow the observation of the electrochromism of PB. This work presents the construction of PB-based, electrochromic screen-printed biosensors. Although electrically more resistive than their graphite counterparts, these new PB-based electrodes enable both the amperometric and colorimetric detection of hydrogen peroxide. This is the first time that this has been achieved using screen-printed electrodes, and we demonstrate it spectroelectrochemically on a glucose biosensor. The biosensor electrochemical performance equals that of previously reported PB/graphite electrodes, being able to detect down to 4  $\mu\text{M}$   $\text{H}_2\text{O}_2$  and 54  $\mu\text{M}$  glucose. At the same time, and in contrast to PB/graphite electrodes, the new PB-based electrodes afford the optical detection of these two analytes down to 1.2  $\mu\text{M}$  and 15  $\mu\text{M}$ , respectively. The dynamic ranges of the glucose biosensors obtained at the PB-based electrodes are 0.1–1 mM (amperometric) and 0.025–2.5 mM (Colorimetric), matching the physiological glucose concentration range in body fluids other than blood or serum.

## 1. Introduction

Prussian Blue consists of iron (II) and (III) atoms bridged by cyanide groups in a cubic crystal structure of formula  $\text{Fe}_4^{3+}[\text{FeII}(\text{CN})_6]_3$ . This composition and structure bestow Prussian Blue its characteristic colour and electrochemical properties. Prussian Blue undergoes two reversible redox reactions, each associated with an ion exchange step and its respective colour change. Thus, Everitt's salt, the reduced form, is colourless  $\text{K}_4\text{Fe}_4^{2+}[\text{FeII}(\text{CN})_6]_3$ , while the oxidized form is yellowish and known as Berlin Green,  $\text{Fe}_4^{3+}[\text{FeIII}(\text{CN})_6]\text{A}$ , where A represents an anion inserted in the crystal lattice to balance charge in the oxidation process. In addition to its electrochromic behavior, that makes it suitable for the fabrication of displays and smart glass [1], Prussian Blue also displays excellent catalytic properties for the reduction of oxygen and hydrogen peroxide. Specifically, this is enabled by the high-spin  $\text{Fe}^{2+}$  atoms in the reduced form [2], which makes Prussian Blue films more active towards  $\text{H}_2\text{O}_2$  reduction than Pt electrodes, and only slightly less active than peroxidase enzymes [3].

This ability to selectively catalyze the reduction of  $\text{H}_2\text{O}_2$  has been successfully exploited in first generation oxidase-based electrochemical [4] and optical [5] biosensors. Karyakin et al. were first to demonstrate

the construction of such biosensors [3,4]. Since then, the number of reports featuring Prussian Blue as artificial peroxidase has increased continuously [6–9]. Surprisingly, despite its electrochromism and sensing capabilities, very few works report the exploitation of its electrochromism for (bio)sensing purposes, and those that do usually rely on PB electrodeposited on expensive transparent electrodes [10–14].

Table 1 provides a summary of key works featuring screen-printed electrodes (SPEs) modified with PB which are used for the amperometric detection of hydrogen peroxide for biosensing purposes, including this work.

Regarding the preparation of PB-modified electrodes, there are three main ways: electrodeposition, chemical growth on an electrode surface, and deposition of PB-modified graphite pastes. Of these, since it was first reported by Neff [27], electrodeposition has been the preferred method when it comes to developing electrochromic devices and electrochemical sensors. The main advantages of electrodeposition methods are not only the selective growth on electrode surfaces alone, but also the control of growth conditions. This ultimately means controlling device-critical features such as film thickness, roughness, porosity, and stability [28]. Deposition methods based on potentiostatic [17], galvanostatic [27], cyclic [3], and pulse voltammetry [29] control have

\* Corresponding author.

E-mail address: [javier.delcampo@csic.es](mailto:javier.delcampo@csic.es) (F.J. del Campo).

<https://doi.org/10.1016/j.snb.2019.03.100>

Received 10 January 2019; Received in revised form 28 February 2019; Accepted 24 March 2019

Available online 05 April 2019

0925-4005/ © 2019 Elsevier B.V. All rights reserved.

**Table 1**

Comparison of different Prussian-Blue screen-printed sensors and biosensors used in the amperometric determination of H<sub>2</sub>O<sub>2</sub>. DS stands for commercial Dropsens SPEs and GNT for electrodes fabricated with a screen-printing paste from Gwent Ltd, UK.

Electrode	Preparation of PB	Analyte	LOD	Range	Sensitivity	Reference
PB on GC	electrodeposition	Glucose	1 $\mu$ M	1 $\mu$ M–5 mM	0.18 A cm <sup>-2</sup> M <sup>-1</sup>	[3]
PB/PPy on C	electrodeposition	Glucose	0.1 mM	0.1–20 mM	1.0–1.9 $\mu$ A cm <sup>-2</sup> mM <sup>-1</sup>	[15]
PB on ITO	electrodeposition	Lactic acid	1 mM	1–20 mM	Unreported	[16]
PB (unspecified electrode)	electrodeposition	H <sub>2</sub> O <sub>2</sub>	0.1 $\mu$ M	0.1 $\mu$ M–0.1 mM	0.6 A cm <sup>-2</sup> M <sup>-1</sup>	[17]
Modified carbon paste	growth on graphite	Glutamate	0.1 $\mu$ M	0.1–100 $\mu$ M	0.21 A cm <sup>-2</sup> M <sup>-1</sup>	[18]
		H <sub>2</sub> O <sub>2</sub>	0.5 $\mu$ M	0.5 $\mu$ M–5 mM	0.11 A cm <sup>-2</sup> M <sup>-1</sup>	
		Glucose	100 $\mu$ M	0.1–10 mM	5.6 $\times 10^{-4}$ A cm <sup>-2</sup> M <sup>-1</sup>	
Screen-printed electrode (DS)	undisclosed	Uric acid	3 $\mu$ M	10–200 $\mu$ M	0.89 A cm <sup>-2</sup> M <sup>-1</sup>	[19]
Screen-printed electrode (DS)	undisclosed	Catechol	0.4 $\mu$ M	1–90 $\mu$ M	Unreported	[20]
Screen-printed electrode (DS)	undisclosed	Paraoxon	12 $\mu$ M	5–150 $\mu$ M	Unreported	[21]
Screen-printed electrode (DS)	undisclosed	Ethanol	20 $\mu$ M	0.05–0.5 mM	0.015 A cm <sup>-2</sup> M <sup>-1</sup>	[22]
Screen-printed electrode (DS)	undisclosed	Glucose	Unreported	0–33.1 mM	5.8 $\times 10^{-4}$ A cm <sup>-2</sup> M <sup>-1</sup>	[23]
Screen-printed electrode (GNT)	undisclosed	H <sub>2</sub> O <sub>2</sub>	3.6 $\mu$ M	0–100 $\mu$ M	0.1 A cm <sup>-2</sup> M <sup>-1</sup>	[24]
		Glucose	0.7 mM	0–100 mM	4.8 $\times 10^{-3}$ A cm <sup>-2</sup> M <sup>-1</sup>	
		Lactate	1.19 mM	0–50 mM	3.0 $\times 10^{-3}$ A cm <sup>-2</sup> M <sup>-1</sup>	
		Uric acid	4.6 mM	0–35 mM	4.5 $\times 10^{-4}$ A cm <sup>-2</sup> M <sup>-11</sup>	
		Lactate	0.15 $\mu$ M	0.15 $\mu$ M–1.1 mM	0.4 A cm <sup>-2</sup> M <sup>-1</sup>	
Screen-printed electrode (GNT)	undisclosed					[25]
Carbon SPE	PB drop casted on C-SPE	Cysteine	98.9 $\mu$ M	300–700 $\mu$ M	0.06 A cm <sup>-2</sup> M <sup>-1</sup>	[26]
PB/Carbon SPE	PB incorporated to C-paste	Cysteine	67.4 $\mu$ M	100–600 $\mu$ M	0.09 A cm <sup>-2</sup> M <sup>-1</sup>	[26]
SiO <sub>2</sub> -ATO/PB	Growth of particles	H <sub>2</sub> O <sub>2</sub>	3.8 $\mu$ M	0.025–5 mM	0.07 A cm <sup>-2</sup> M <sup>-1</sup>	This work
ITO/PB <sup>2</sup>	Growth of particles	H <sub>2</sub> O <sub>2</sub>	3.2 $\mu$ M	0.01–5 mM	0.08 A cm <sup>-2</sup> M <sup>-1</sup>	This work
SiO <sub>2</sub> -ATO/PB	Growth of particles	Glucose	54.1 $\mu$ M	0.1–1 mM	8.8 $\times 10^{-3}$ A cm <sup>-2</sup> M <sup>-1</sup>	This work
ITO/PB	Growth of particles	Glucose	70.5 $\mu$ M	0.1–1 mM	7.4 $\times 10^{-3}$ A cm <sup>-2</sup> M <sup>-1</sup>	This work

<sup>1</sup>SiO<sub>2</sub>-ATO/PB: Prussian Blue was chemically grown on SiO<sub>2</sub> core and ATO-shell 3  $\mu$ m particles.

<sup>2</sup> ITO/PB: Prussian Blue was chemically grown directly on 100 nm ITO nanoparticles.

been reported. PB is typically electrodeposited from solutions containing Fe(III) and ferricyanide ions. However, electrodeposition from Fe(II) and ferrocyanide is also possible and may be desirable when a less acidic pH is required to preserve the activity of enzymes or other biomolecules [15].

Chemical growth, on the other hand, may also be used to produce Prussian Blue films, both on electrodes [26,30,31] and on inert surfaces [32] in many different ways [33]. However, this is not an ideal approach because it lacks the surface selectivity and much of the control that electrochemical methods enjoy.

Nevertheless, chemical synthesis of PB is used in the formulation of screen-printing materials, which is the third relevant approach that we have identified for the production of PB-modified electrodes.

Up until the mid 1990s, most electrochemical studies on Prussian Blue used electrodeposited films. However, the use of chemically synthesized Prussian Blue has been made popular through the introduction of carbon paste [34] and screen-printed electrodes [35] (SPEs). PB-modified pastes represent a straightforward way to overcome critical production issues affecting electrodeposition, such as the batch nature of the electrodeposition process and its relatively high cost. Screen-printing also extends the nature of possible substrates beyond conducting electrode materials, to include paper, textiles, ceramics, polymers and, given the right combination of solvents and curing conditions, nearly any material imaginable.

PB-mediated pastes have typically three key components: a conducting material, the PB itself, and a suitable binder system. The conducting material used in existing commercial products is graphite, and different resins are used as binder agents.

In this work, we have grown PB chemically over the surface of clear conducting particles, and then mixed the modified particles with a Viton® binder system to produce an electrochromic paste. This material had been previously reported for the construction of electrochromic displays [36] but, to the best of our knowledge, this is its first demonstration in (bio)sensing. Thus, in contrast to previously reported PB/graphite-based screen-printed electrodes, which are limited to electrochemical detection only, the electrodes presented here enable both electrochemical and optical detection of H<sub>2</sub>O<sub>2</sub>. The electrochemical performance of the materials presented here is comparable to

graphite-based materials, but their electrochromism makes them very attractive also for the construction of optical (bio)sensors. This concept is demonstrated in the context of a glucose oxidase-based biosensor.

## 2. Experimental

### 2.1. Reagents and materials

Potassium ferrocyanide, ferrous sulfate, potassium chloride, acetic acid, glucose, bovine serum albumin (BSA), and 2-butoxyethyl acetate were purchased from Sigma-Aldrich. Glucose oxidase (236 U mg<sup>-1</sup>) was acquired from Sekisui Diagnostics (UK). Chitosan (M.W. 100,000–300,000) was purchased from Acros Organics. SiO<sub>2</sub>-ATO conducting particles (nominal size of 3  $\mu$ m) Zelec 1610-S were kindly provided by Milliken Chemical (BE). ITO conducting particles (nominal size of 50 nm), NanoTek®, were purchased from Alfa Aesar. Viton® fluoroelastomer (GBL-600S, DuPont) was acquired from Eagle Elastomer (USA). Carbon conducting paste ref. C2030519P4 and PB-modified carbon paste ref. C2070424P2 were purchased from Gwent Electronic Materials, Ltd (UK). Electrodag PF-455B photocurable dielectric and 725A silver pastes were obtained from Henkel (ES). 0.5 mm-thick PET sheets (Autostat WP20) were purchased from MacDermid (UK). PB-modified screen-printed carbon electrodes (PB-SPEs) ref. 710 were purchased from Dropsens (ES).

All chemicals were used as received without further purification.

### 2.2. Instrumentation

Electrochemical and spectroelectrochemical measurements were done using a SPELEC instrument (Dropsens) controlled by DropView SPELEC software (version 3.0), installed on a PC running Windows 10. Scanning electron microscopy images were obtained at an Auriga microscope (Carl Zeiss). A Kulik&Soffa four-point probe connected to a 3455A Digital Voltmeter (Hewlett Packard) was used to measure the sheet resistance of the fabricated materials.

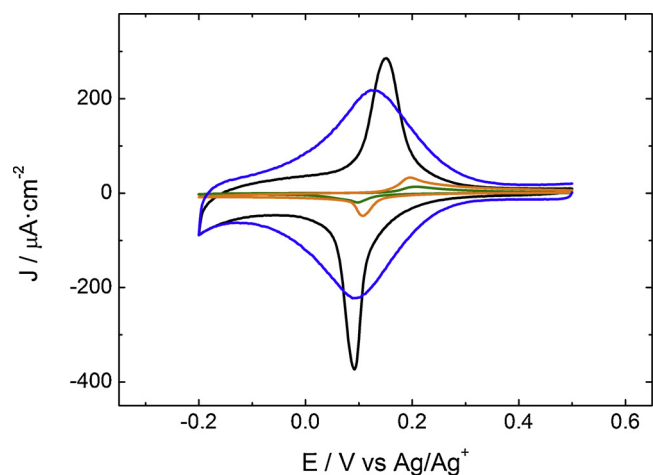


**Fig. 1.** Cyclic voltammograms obtained in supporting electrolyte for the different types of PB-SPEs. Scan rate of  $5 \text{ mVs}^{-1}$ .  $\text{SiO}_2\text{-ATO/PB}$  (Black),  $\text{ITO/PB}$  (Blue), DropSens C/PB (Orange), Gwent C/PB (Green). (For interpretation of the references to colour in the text, the reader is referred to the web version of this article.)

### 2.3. Electrochromic Prussian Blue screen-printed electrodes

Prussian Blue screen-printing pastes were prepared following a previously published protocol [36]. Briefly, 20 g of conducting ITO or  $\text{SiO}_2\text{-ATO}$  particles were suspended, under vigorous stirring, in 200 mL of a 25 mM iron (II) sulfate aqueous solution. Then, 30 mL of a 60 mM ferricyanide solution were added dropwise to the stirred solution. The resulting blue particles were separated by decantation, washed with dilute HCl, and dried at  $100^\circ\text{C}$ .

Prussian Blue-modified conducting particles were next combined with a 15–20% Viton solution prepared in 2-butoxyethylacetate to a 5:2 pigment to binder proportion, and thoroughly mixed in a ball mill, until the resulting paste presented a honey-like texture. The particle size was measured using a  $50 \mu\text{m}$  grind gauge, obtaining a maximum particle size range between 5 and  $12 \mu\text{m}$ . This is extremely good considering that the starting particle size was nominally  $3 \mu\text{m}$ , and that no additives were used to promote particle suspension in the paste.

Due to the high electrical resistance of the printed Prussian Blue layers, it was needed to print it over a conducting substrate. The simplest and most cost-effective case involved its application over a graphite screen-printed electrode. However, to enhance the colour contrast of the electrochromic change, a  $\text{SiO}_2\text{-ATO}$  layer [37] was additionally printed between the graphite and the Prussian Blue layers. All the electrodes presented in this work have been prepared as previously reported, using a manual, home-made screen printing setup [38].

### 2.4. Glucose biosensor fabrication

Prussian Blue screen-printed electrodes (PB-SPEs) were modified following a modified version of a previously reported protocol [39]. Briefly,  $4 \mu\text{L}$  of a 0.5% wt. chitosan solution prepared in 0.1 M acetic acid was cast on the surface of the electrodes and allowed to dry at room temperature. The electrodes were subsequently rinsed with deionized water, and  $6 \mu\text{L}$  of a  $5 \text{ mg mL}^{-1}$  GOx containing  $15 \text{ mg mL}^{-1}$  BSA were then cast and allowed to dry. The electrodes were stored at  $4^\circ\text{C}$ .

### 2.5. Electrochemical measurements

All the experiments were carried out in a 50 mM phosphate buffered solution and 0.1 M KCl, adjusted to a pH of 5.5. The selected pH ensures the stability of the Prussian Blue while keeping the activity of the

oxidase enzymes on the electrode near their optimum activity. For the electrochemical characterization, the electrodes were preconditioned by cyclic voltammetry, applying 20 cycles at a scan rate of  $20 \text{ mVs}^{-1}$ , to equilibrate the crystalline structure of the Prussian Blue with the  $\text{K}^+$  cations in the supporting electrolyte [17]. Note, however, that no preconditioning step was required for the sensing of hydrogen peroxide or glucose.

Limits of detection, LoD have been determined based on conventional  $3\sigma/m$  methodology, where  $\sigma$  corresponds to the background signal standard deviation, and  $m$  to the slope of the linear range [40].

### 2.6. Spectroelectrochemical measurements

Reflectance measurements were done using DropSens-SPELEC reflectance cell, using solutions of same composition as those described in Section 2.4 above. The dark spectrum was recorded with the optical shutter closed. Background spectra were recorded over completely reduced electrodes, which displayed the clearest colour. Unless otherwise stated, spectra were collected using an integration time of 300 ms. Data analysis was carried out using SPELEC DropView software.

## 3. Results and discussion

### 3.1. Characterization of Prussian Blue electrodes

The electrochemical and spectroelectrochemical performance of the PB-SPEs was evaluated and compared to that of (i) electrodes fabricated with a commercial PB-Graphite paste, and (ii) to commercial PB-SPEs. For the sake of clarity and simplicity, from here on we will refer to these as “commercial materials” and “graphite electrodes” indistinctively, and to ours as “electrochromic pastes” or “PB-electrodes”.

Fig. 1 shows cyclic voltammograms recorded in supporting electrolyte. The most striking difference in the voltammetry of the different PB-modified pastes is the much higher currents observed for the blue pastes presented here, compared to those obtained from the commercial materials. One feature of ITO nanoparticles compared to  $\text{SiO}_2\text{-ATO}$  particles is that pastes with significantly higher particle to binder ratios can be formulated, so even higher PB loadings could, in principle be achieved, but the significantly higher cost of ITO nanoparticles compared to  $\text{SiO}_2\text{-ATO}$  particles should also be considered.

The cyclic voltammograms in Fig. 1 suggest that commercial graphite pastes contain a much lower amount of Prussian Blue than the electrochromic pastes presented here. Also, the voltammograms in Fig. 1 show that our PB-based electrodes display relatively larger background currents. Note that similarly high background currents have been observed for electrodes made with unmodified ATO particles [37], but also on sol-gel-derived Prussian Blue-silicate electrodes [10]. We believe there are two likely reasons for such currents; first, the porous structure and resulting large surface area of the electrodes (see Fig. S1), but also, in the present case, the mild electroactivity of indium and antimony tin-oxides [41,42].

The PB-electrodes presented here exhibit a superior electrochemical behavior based on their peak-to-peak separation compared to commercial materials based on graphite (Table S1). This is probably due to a better contact of the PB and the conducting material. ITO-modified nanoparticles display the smallest peak-to-peak separation, ca. 30 mV at  $5 \text{ mVs}^{-1}$ , presumably due to the better conductivity afforded by ITO nanoparticles compared to  $\text{SiO}_2\text{-ATO}$  micro-particles. However, the much higher PB loading, arising from the massive available surface area of the nanoparticles combined with the thickness of the screen-printed layer, results in much broader peaks compared to the other materials. This peak broadness, which may be detrimental for electroanalytical applications, is due to a limitation in the rate of potassium exchange during the redox process. In fact, this limitation has been observed for all 4 electrode types under study in the form of linear plots of peak current vs. square root of scan rate (Fig. S2). Such a linear dependency

points at a diffusion controlled process, where the only diffusing species involved here are potassium cations. In contrast, thin film electro-generated PB electrodes [43,44] exhibit a surface-controlled regime as predicted by the Laviron expression [45]. The reason for this different behavior is in the thickness of the PB layer. While electrodeposited layers are typically in the range of nanometers (hundreds), screen printed layers are at least a few microns thick and can exchange larger amounts of cations. In all cases, charge densities have been calculated using the electrode geometric area, which allows for a very limited comparison as the thickness of the PB coating on the screen-printed electrodes is unknown. Therefore, although the actual surface area of our screen-printed electrodes has not been determined, the charge density analysis of the PB peak at the different electrodes shows that our PB-based electrodes contain between 5 and 7 times more Prussian Blue than an electrodeposited layer (See Table S1).

Another important difference between graphite-PB and the  $\text{SiO}_2$ -ATO/ITO-PB-electrodes is their electrical conductivity. We found, using four-point probe measurements of test structures, that the resistivity of Prussian Blue modified particles increases by more than 5 times compared to a paste of unmodified particles at the same concentration (see Table S2). This suggests that commercial materials may have been produced simply by adding PB particles to an existing graphite paste formulation, which could also explain their smaller PB signals, and their somewhat broader peak-to-peak separation in the voltammetry.

Next, the spectroelectrochemical response of the PB-SPEs was compared. The black colour of graphite in the commercial PB-modified commercial electrodes precluded the observation of any spectroelectrochemical changes, in contrast with the ITO and ATO based pastes presented here. Fig. 2A and B shows cyclic voltammograms of the two types of PB-SPEs together with the derivative of their respective voltabsorptograms. A clear correlation between the electrochemical and the spectroscopic behavior of these electrodes is apparent, although a

shift ca. 50 mV is observed between the two signals in ITO/PB electrodes. This shift in peak position between electrochemical and optical signals has been reported in the past and, again, is attributed to the mass transport limitations of  $\text{K}^+$  exchange from the Prussian Blue lattice, and which is involved in the colouration process [34]. In spite of this slight delay between the current and the colour change, neither the electrocatalytic performance of the material nor its electrochromism have been adversely affected.

The performance and stability of the electrochromic material under a continuous switching regime was also studied. The potential of the working electrode was stepped between  $-0.1$  and  $+0.4$  V vs.  $\text{Ag}/\text{Ag}^+$  in 60-s intervals in a  $0.25$  mM  $\text{H}_2\text{O}_2$  solution prepared in the supporting electrolyte. The experiment was carried out in the presence of hydrogen peroxide to simulate the conditions of an oxidase-based biosensor where hydrogen peroxide is produced. Fig. 2C shows the change in absorbance as reducing and oxidizing potentials are applied. The data show that ITO/PB electrodes display a higher contrast between the oxidized and reduced states than  $\text{SiO}_2$ -ATO/PB electrodes do. This is mainly due to two reasons. First, the higher PB loading of the ITO nanoparticle-based electrodes, confirmed by the charge densities in Table 1 above, makes these electrodes show a much deeper blue colour than  $\text{SiO}_2$ -ATO based electrodes, and so when Prussian Blue is reduced into the colourless Everitt's salt or Prussian White (PW), the contrast to the pale yellow of the underlying nanoparticles is enhanced. The second reason seems to be a wetting issue of  $\text{SiO}_2$ -ATO-based electrodes. Although both types of electrodes are highly hydrophobic due to the Viton binder (see Table S3),  $\text{SiO}_2$ -ATO-PB electrodes wet more slowly than ITO based electrodes. This is likely due to differences in surface topology and roughness. Eventually, however, the electrolyte wets the entire surface, allowing the interaction between more PB particles and the solution. Although this enables the maximum contrast of the material on electrochromic switching, this is still lower than at PB-ITO

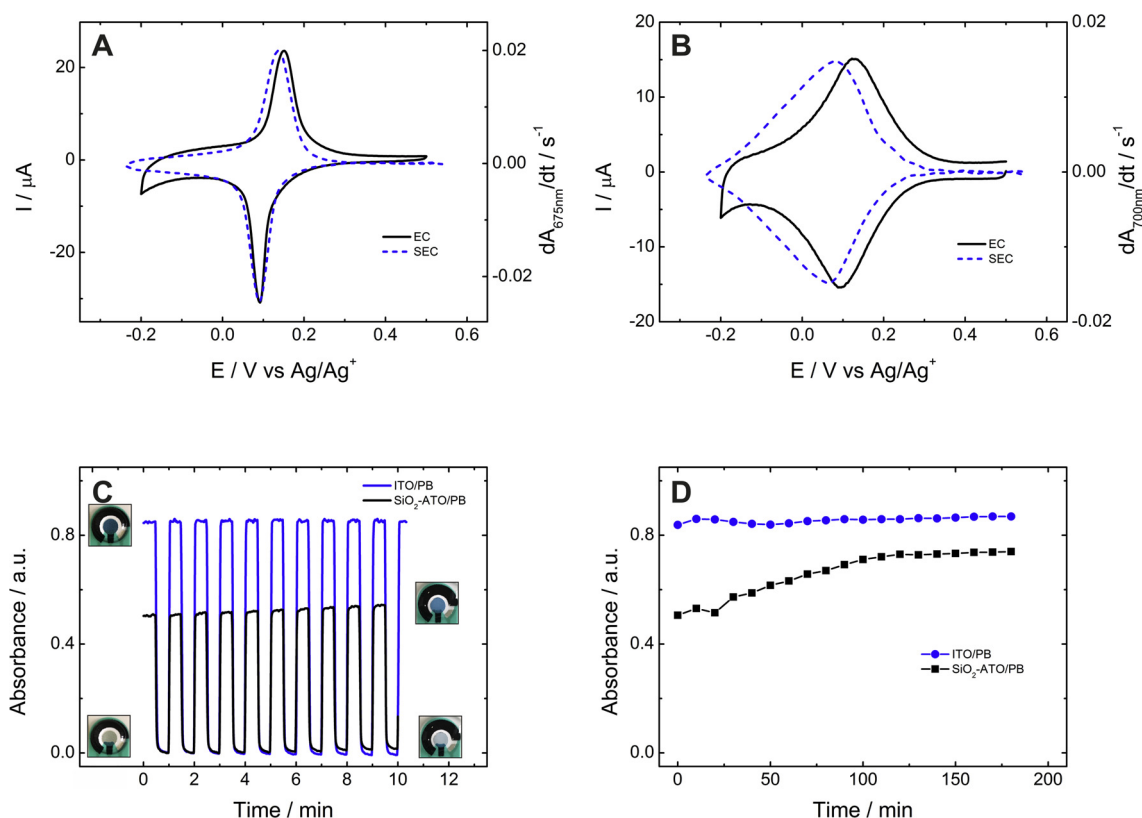


**Fig. 2.** Cyclic voltammogram in supporting electrolyte and derivative of the voltabsorptogram for a  $\text{SiO}_2$ -ATO/PB (a) and ITO/PB (b) electrode. Scan rate  $5 \text{ mVs}^{-1}$ . (c) Plot of the evolution of absorbance when potential was stepped from  $-0.1$  to  $+0.4$  V vs  $\text{Ag}/\text{Ag}^+$  at intervals of 60 s in a  $0.25$  mM  $\text{H}_2\text{O}_2$  solution in supporting electrolyte. (d) Representation of the contrast variation of the experiment in (c) for a longer time scale.



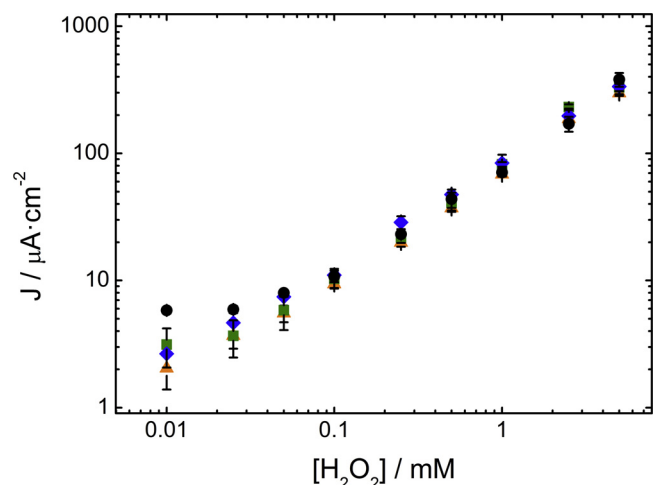


**Fig. 3.** Plot of the current density against the hydrogen peroxide concentration. Applied potential of  $-0.1$  V vs.  $\text{Ag}/\text{Ag}^+$  pseudo-reference electrode. DropSens C/PB (Orange triangles), ITO/PB (Blue diamonds), Gwent C/PB (Green squares), and  $\text{SiO}_2$ -ATO/PB (Black circles). (For interpretation of the references to colour in the text, the reader is referred to the web version of this article.)

nanoparticle-based electrodes.

Fig. 2D shows this gradual contrast increase at  $\text{SiO}_2$ -ATO-PB electrodes, from an initial 0.5 a.u. up to roughly 0.7 a.u.

On the other hand, this effect is not observed when a polymeric layer, such as chitosan in this work, covers the electrochromic material. The chitosan coating seems to wet the electrode surface completely, reducing the hydrophobicity of the material and facilitating the electrode interaction with the test solution (see Table S3).

### 3.2. PB electrodes for $\text{H}_2\text{O}_2$ sensing

The various Prussian Blue electrodes were used in the electrochemical determination of hydrogen peroxide, and their behavior was compared. Electrodes were polarized at a reduction potential of  $-0.1$  V vs Ag, where Prussian White is formed and the catalytic reduction of peroxide takes place.

Fig. 3 shows current density as a function of peroxide concentration for the 4 electrodes tested. In all cases, a linear response is observed between  $25\ \mu\text{M}$  and  $5\ \text{mM}$   $\text{H}_2\text{O}_2$ . The amperometric sensitivities of the four electrode types are very similar, roughly  $0.08\ \text{A cm}^{-2}\ \text{M}^{-1}$ , and detection limits are in the range of  $1\ \mu\text{M}$ – $4\ \mu\text{M}$  (see Table S4). This is in line with other reports on PB-modified graphite electrodes (see Table 1), and indicative of the suitability of these electrodes as an artificial peroxidase for sensing applications, particularly in non-invasive detection systems.

In addition to enabling the amperometric detection of  $\text{H}_2\text{O}_2$ , these PB-based electrodes also allow optical quantification through reflectance spectroscopy. It is surprising that, whilst the electrochemical detection of  $\text{H}_2\text{O}_2$  at Prussian Blue electrodes is amply demonstrated and accepted, there are much fewer examples of optical quantification of  $\text{H}_2\text{O}_2$  at Prussian Blue electrodes, including electrodeposited Prussian Blue layers [5,14,46,47].

The electrochromic properties of the fabricated PB-SPEs were also exploited in the optical quantification of hydrogen peroxide. The measurement was carried out as follows. First, Prussian Blue was reduced to Prussian White at potential of  $-0.1$  V vs. Ag. Once a stable background colorimetric signal was observed, after approximately 60 s of electrode polarization, the potentiostat was switched off, leaving the electrochemical cell at open circuit. Then, the peroxide in the solution chemically oxidized the Prussian White back to Prussian Blue, and the corresponding colour change was monitored by UV–vis reflectance (Fig. 4A). Maximum colour contrast depends on the colour of the

underlying conducting particles, which were white or pale yellow respectively. These were found to be  $675\ \text{nm}$  for  $\text{SiO}_2$ -ATO/PB electrodes and  $700\ \text{nm}$  for ITO/PB. Fig. 4B shows plots of absorbance versus time at these wavelengths, as a means to monitor the hydrogen peroxide reduction at the PW/PB surface. As the data show, the higher the  $\text{H}_2\text{O}_2$  concentration, the faster the electrode recovers its blue colour fully. Fig. 4C shows the relation between peroxide concentration and reflectance measured at  $700\ \text{nm}$ , 100 s after electrode depolarization. In a manner akin to coulometric sensors, which sensitivity and detection limit can be adjusted by choosing a suitable (current) integration time, here the sensor performance can be adjusted to the sample concentration simply by adjusting the integration time of the spectrophotometer and/or the sampling time after electrode depolarization (in our case 300 ms and 100 s, respectively). This provides control over the sensitivity, linear range or detection limit of the method (Table S5).

Longer experimental times result in markedly increased sensitivities, and consequently lower detection limits. Moreover, the sensor dynamic ranges also vary, so the technique can be easily adjusted to match a sample expected concentration, and thus improve the reliability of the measurement.

Note that, although dissolved oxygen is also able to oxidize Prussian White back to Prussian Blue, the rate of this reaction is considerably slower than the peroxide driven oxidation, and so its effect may be ignored and the process considered selective towards peroxide, barring cases of extremely low peroxide concentration.

When comparing the two PB-based electrochromic electrodes, ITO electrodes display higher absorbances and sensitivity values than ATO-based electrodes. This may be due to the higher amount of electrochromic material present in the paste which enhances the colour contrast between the reduced and oxidized states of the material (see Table S1).

Tables S4 and S5 show that the optical method is slightly more sensitive. Controlling integration and sampling times in the spectroscopic detection lets the user modify the sensitivity of the measurement and adjust it to the specific requirements of the application. This makes this approach a powerful and versatile basis for the design of enzymatic biosensors.

### 3.3. Electrochromic glucose biosensor

Once the suitability of the PB-SPEs as a sensing platform for hydrogen peroxide was established, a glucose biosensor based on glucose oxidase was prepared. The enzymatic oxidation of glucose yields hydrogen peroxide which, at the PB-modified electrodes, enables the quantification of glucose both electrochemically and spectroscopically.

Fig. 5a shows the amperometric Michaelis-Menten plots for glucose using the two fabricated electrochromic PB-SPEs. The dynamic range of both biosensors is slightly shorter than other reported biosensors (see Table 1), ranging from 0.1 to 1 mM glucose and reaching saturation above 2.5 mM. We believe that at this point the amount of hydrogen peroxide produced by the oxidase inhibits the enzymatic activity of GOx. This could be solved by improving the fabrication of the glucose biosensor, using different polymeric membranes and/or stabilizing agents to control the diffusion of the analyte through the biosensor, and to increase the operational stability of the enzyme [48]. On the other hand, the analytical performance of our blue biosensors in terms of detection limit and sensitivity, ca.  $60\ \mu\text{M}$  and  $8 \cdot 10^{-3}\ \text{A cm}^{-2}\ \text{M}^{-1}$  (see Table S6), is comparable to that of other reported amperometric biosensors (see Table 1).

The maximum current densities registered for the glucose biosensors can be extrapolated to the hydrogen peroxide calibration plot in Fig. 3 to have an estimation of the amount of hydrogen peroxide produced in the enzymatic reaction. A value of  $0.25\ \text{mM}$   $\text{H}_2\text{O}_2$  is obtained, which in the spectroscopic experiment would generate an absorbance of roughly 0.1 a.u. To increase this absorbance value, and also the sensitivity of the glucose sensor, the sampling time in the spectroscopic

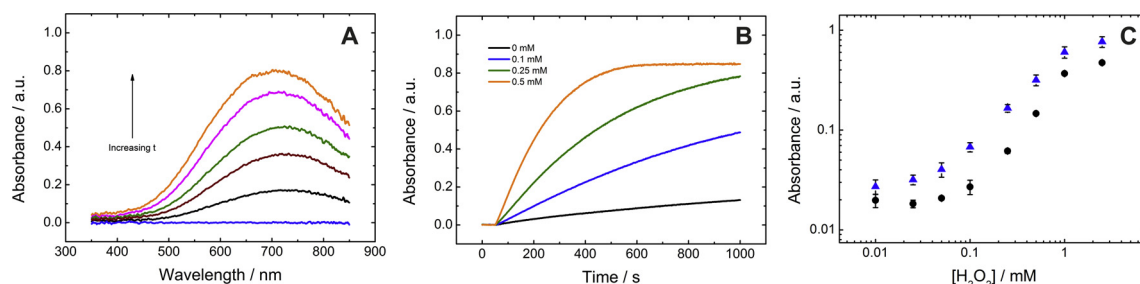


**Fig. 4.** (a) Progress with time of the absorbance spectra for an ITO/PB electrode in a 0.25 mM  $H_2O_2$  solution in supporting electrolyte. (b) Evolution of the absorbance measured at 700 nm with time for different hydrogen peroxide concentrations in an ITO/PB electrode (see Figure S3 for the plots in (a) and (b) obtained with a SiO<sub>2</sub>-ATO/PB electrode). (c) Plots of the absorbance measured at 700 nm for a fixed time of 100 s in ITO/PB (Blue triangles) and SiO<sub>2</sub>-ATO/PB (Black circles) electrodes. Error bars represent the standard deviation for three different electrodes. (For interpretation of the references to colour in the text, the reader is referred to the web version of this article.)

determination was modified from 100 s to 300 s.

Fig. 5b shows the spectroscopic calibration plots of the glucose biosensor for the two different PB-SPEs. As seen, no substantial differences are observed when either the amperometric or the spectroscopic detection method is used, as a similar dynamic range is achieved in all cases, reaching in both cases a plateau at concentrations higher than 2.5 mM. A slight gain in the detection limit is achieved as it decreases up to roughly 15  $\mu$ M likely due to the effect of the high background currents present in the amperometric detection that disappear when a spectroscopic detection method is used but, all in all, the performance of both types of electrochromic electrodes is comparable, regardless of the detection method employed.

#### 4. Conclusions and outlook

We have presented a new kind of electrochromic, Prussian Blue based screen-printed sensors suitable for spectroelectrochemical detection. To the best of our knowledge, this is the first report of a screen-printed electrochromic paste applied to sensing and biosensing.

The Prussian Blue electrochromic pigment used is prepared by chemically growing a thin PB layer on the surface of two different kinds of tin oxide-based conducting particles, namely 50–100 nm indium tin oxide (ITO) nanoparticles, and 3  $\mu$ m SiO<sub>2</sub> particles covered by a thin (ca. 100 nm) antimony tin oxide (ATO) shell. These PB-modified pigments, combined with a Viton® binder system, yield high-quality screen-printing pastes. However, the high electrical resistance of the resulting layers required printing the material on a conventional electrode surface. Also, to increase the colour contrast further, an undercoat of a similar SiO<sub>2</sub>-ATO paste was printed underneath the blue coating and over a graphite electrode.

The electrocatalytic response of these blue pastes toward the reduction of hydrogen peroxide is in line with that of the commercial PB-modified screen-printed electrodes and materials. However, in contrast to these, the materials presented here also enable the optical detection and quantification of hydrogen peroxide in the  $\mu$ M–mM range, which represents a clear advantage and opens new avenues for the design of novel multi-functional spectroelectrochemical devices.

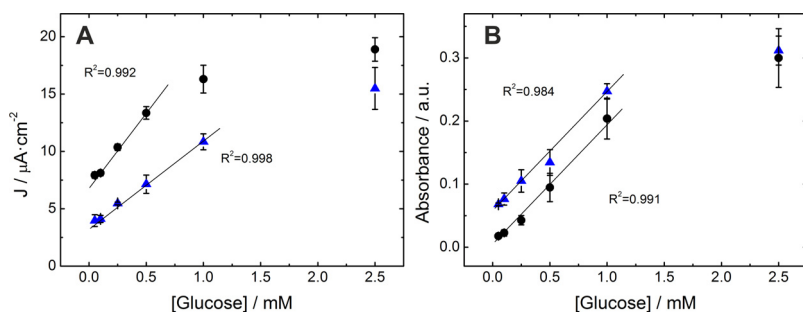


**Fig. 5.** (a) Amperometric and (b) spectroscopic calibration curves for the glucose biosensor obtained with ITO/PB (Blue triangles) and SiO<sub>2</sub>-ATO/PB (Black circles) electrodes. Error bars represent the standard deviation of three different electrodes. (For interpretation of the references to colour in the text, the reader is referred to the web version of this article.)

These electrochromic sensors pose important advantages compared to both electrodeposited PB and screen-printed PB-modified graphite electrodes. They overcome electrodeposition limitations, such as (i) the “wet” nature of the process, (ii) the need to control critical electrodeposition parameters such as current and potential distribution over large area substrates, and (iii) it replaces an intrinsically “batch” process by a “continuous” large area process, screen-printing. On the other hand, compared to currently available PB-modified graphite pastes, the materials presented here enable the use of both electrochemical and optical detection, opening new design avenues. One possible direction would be the development of multiparametric devices based on arrays of electrochromic electrodes. A smart example of this has been recently presented by Zhang and Liu where lactic acid can be quantitatively determined by the naked eye [16].

Although in this work we have printed these electrochromic electrodes over graphite transducers, printing them over transparent electrodes would provide additional advantages, such as the possibility to observe the colour change from the back a transparent substrate. Although analysis of coloured samples, such as blood, may be more challenging, one way to keep the colour contrast would be to protect the electrochromic electrode with a white semipermeable coating or membrane. In any case, the possibility to screen-print electrochromic electrodes widely opens the range of possible applications for electrochromism in analytical chemistry, including non-invasive sensors and smart sensing tags in food packaging, and even gas sensors.

Last, this work has focused on the use of PB as model electrochrome. However, other electrochromic materials, including conducting polymers [49,50], which have also been used in the construction of electrochromic sensors, could also be used in the mass production of new sensors using the approach presented here to formulate related screen-printing materials.

#### Acknowledgements

MA is supported by FEDER funds managed by the Catalan Secretary of Universities and Research through project PROD-0000114 (Enterprise and Knowledge, Industry Department, Generalitat de

Catalunya). JdC gratefully acknowledges financial support through a 2016 Leonardo grant from the BBVA Foundation. The authors are grateful to Milliken for providing the electroconductive powders (ECPs) featured in this work. Zelec materials by Milliken provide cost-effective, static-dissipative performance for coatings and polymers. They are non-volatile, non-corrosive, and resistant to heat, chemicals and humidity. Zelec enhances quality and durability by imparting resistivity throughout the lifetime of coatings, paints, security inks and electronics products.

## References

- [1] R.J. Mortimer, D.R. Rosseinsky, P.M.S. Monk, *Electrochromic Materials and Devices*, Wiley-VCH, Weinheim, Germany, 2015.
- [2] K. Itaya, N. Shoji, I. Uchida, Catalysis of the reduction of molecular oxygen to water at Prussian Blue modified electrodes, *J. Am. Chem. Soc.* 106 (1984) 3423–3429.
- [3] A.A. Karyakin, O.V. Gitelmacher, E.E. Karyakina, A high-sensitive glucose amperometric biosensor based on Prussian Blue modified electrodes, *Anal. Lett.* 27 (1994) 2861–2869.
- [4] A.A. Karyakin, O.V. Gitelmacher, E.E. Karyakina, Prussian Blue-based first-generation biosensor. A sensitive amperometric electrode for glucose, *Anal. Chem.* 67 (1995) 2419–2423.
- [5] R. Koncki, T. Lenarczuk, A. Radomska, S. Głab, Optical biosensors based on Prussian Blue films, *Analyst* 126 (2001) 1080–1085.
- [6] Q. Chi, S. Dong, Amperometric biosensors based on the immobilization of oxidases in a Prussian Blue film by electrochemical codeposition, *Anal. Chim. Acta* 310 (1995) 429–436.
- [7] A.A. Karyakin, E.E. Karyakina, L. Gorton, Prussian-Blue-based amperometric biosensors in flow-injection analysis, *Talanta* 43 (1996) 1597–1606.
- [8] S.A. Jaffari, J.C. Pickup, Novel hexacyanoferrate (III)-modified carbon electrodes-application in miniaturized biosensors with potential for in vivo glucose sensing, *Biosens. Bioelectron.* 11 (1996) 1167–1175.
- [9] J. Kim, J.R. Sempionatto, S. Imani, M.C. Hartel, A. Barfidokht, G. Tang, et al., Simultaneous monitoring of sweat and interstitial fluid using a single wearable biosensor platform, *Adv. Sci.* (2018) 1800880.
- [10] S. Bharathi, O. Lev, Sol-gel-derived Prussian Blue-silicate amperometric glucose biosensor, *Appl. Biochem. Biotechnol.* 89 (2000) 209–216.
- [11] K.-S. Tseng, L.-C. Chen, K.-C. Ho, Amperometric detection of hydrogen peroxide at a Prussian Blue-modified FTO electrode, *Sens. Actuators B: Chem.* 108 (2005) 738–745.
- [12] L. Chen, K. Ho, Multimode optoelectrochemical detection of cysteine based on an electrochromic Prussian Blue electrode, *Sens. Actuators B: Chem.* 130 (2008) 418–424.
- [13] P. Virbickas, A. Valiūnienė, A. Ramanavičius, Towards electrochromic ammonium ion sensors, *Electrochem. commun.* 94 (2018) 41–44.
- [14] A. Złoczewska, A. Celebanska, K. Szot, D. Tomaszewska, M. Opallo, M. Jonsson-Niedziolka, Self-powered biosensor for ascorbic acid with a Prussian Blue electrochromic display, *Biosens. Bioelectron.* 54 (2014) 455–461.
- [15] A. Ramanavičius, A.I. Rekertaitė, R. Valiūnas, A. Valiūnienė, Single-step procedure for the modification of graphite electrode by composite layer based on polypyrrole, Prussian Blue and glucose oxidase, *Sens. Actuators B: Chem.* 240 (2017) 220–223.
- [16] F. Zhang, T. Cai, L. Ma, L. Zhan, H. Liu, A paper-based electrochromic array for visualized electrochemical sensing, *Sensors (Basel)* 17 (2017).
- [17] A.A. Karyakin, E.E. Karyakina, Prussian Blue-based 'artificial peroxidase' as a transducer for hydrogen peroxide detection. Application to biosensors, *Sens. Actuators B: Chem.* 57 (1999) 268–273.
- [18] D. Moscone, D. D'Ottavi, D. Compagnone, G. Palleschi, Construction and analytical characterization of Prussian Blue-based carbon paste electrodes and their assembly as oxidase enzyme sensors, *Anal. Chem.* 73 (2001) 2529–2535.
- [19] F.S. da Cruz, Fd.S. Paula, D.L. Franco, W.T.P. dos Santos, L.F. Ferreira, Electrochemical detection of uric acid using graphite screen-printed electrodes modified with Prussian Blue/poly(4-aminosalicylic acid)/uricase, *J. Electroanal. Chem.* 806 (2017) 172–179.
- [20] M. Buleandra, A.A. Rabinca, C. Mihailciuc, A. Balan, C. Nichita, I. Stamatin, et al., Screen-printed Prussian Blue modified electrode for simultaneous detection of hydroquinone and catechol, *Sens. Actuators B* 203 (2014) 824–832.
- [21] V. Scognamiglio, I. Pezzotti, G. Pezzotti, J. Cano, I. Manfredonia, K. Buonasera, et al., Towards an integrated biosensor array for simultaneous and rapid multi-analysis of endocrine disrupting chemicals, *Anal. Chim. Acta* 751 (2012) 161–170.
- [22] E. Costa Rama, J. Biscay, M.B. Gonzalez Garcia, A. Julio Reviejo, J.M. Pingarron Carrazon, A. Costa Garcia, Comparative study of different alcohol sensors based on screen-printed carbon electrodes, *Anal. Chim. Acta* 728 (2012) 69–76.
- [23] J. Noiphung, T. Songjaroen, W. Dungchai, C.S. Henry, O. Chailapakul, W. Laiwattanapaisa, Electrochemical detection of glucose from whole blood using paper-based microfluidic devices, *Anal. Chim. Acta* 788 (2013) 39–45.
- [24] W. Dungchai, O. Chailapakul, C.S. Henry, Electrochemical detection for paper-based microfluidics, *Anal. Chem.* 81 (2009) 5821–5826.
- [25] T. Shimomura, T. Sumiya, M. Ono, T. Itoh, T.-A. Hanaoka, An electrochemical biosensor for the determination of lactic acid in expiration, *Procedia Chem.* 6 (2012) 46–51.
- [26] J.A. Bonacin, P.L.D. Santos, V. Katic, C.W. Foster, C.E. Banks, Use of screen-printed electrodes modified by Prussian Blue and analogues in sensing of cysteine, *Electroanalysis* 30 (2017) 170–179.
- [27] V.D. Neff, Electrochemical oxidation and reduction of thin films of Prussian Blue, *J. Electrochem. Soc.* 125 (1978) 886–887.
- [28] C.L. Lin, K.C. Ho, A study on the deposition efficiency, porosity and redox behavior of Prussian Blue thin films using an EQCM, *J. Electroanal. Chem.* 524–525 (2002) 286–293.
- [29] P. Najafisayar, M.E. Bahrololoom, Pulse electrodeposition of Prussian Blue thin films, *Thin Solid Films* 542 (2013) 45–51.
- [30] A.N. Sekretaryova, V. Beni, M. Eriksson, A.A. Karyakin, A.P.F. Turner, M.Y. Vagin, Cholesterol self-powered biosensor, *Anal. Chem.* 86 (2014) 9540–9547.
- [31] E.V. Karpova, E.E. Karyakina, A.A. Karyakin, Communication—accessing stability of oxidase-based biosensors, *J. Electrochem. Soc.* 164 (2017) B3056–B3058.
- [32] S. Cinti, R. Cusenza, D. Moscone, F. Arduini, Paper-based synthesis of Prussian Blue nanoparticles for the development of whole blood glucose electrochemical biosensor, *Talanta* 187 (2018) 59–64.
- [33] B. Kong, C. Selomulya, G. Zheng, D. Zhao, New faces of porous Prussian Blue: interfacial assembly of integrated hetero-structures for sensing applications, *Chem. Soc. Rev.* 44 (2015) 7997–8018.
- [34] N.F. Zakharchuk, B. Meyer, H. Hennig, F. Scholz, A. Jaworski, Z. Stojek, A comparative study of Prussian-Blue-modified graphite paste electrodes and solid graphite electrodes with mechanically immobilized Prussian Blue, *J. Electroanal. Chem.* 398 (1995) 23–25.
- [35] M.P. O'Halloran, M. Pravda, G.G. Guibault, Prussian Blue bulk modified screen-printed electrodes for H<sub>2</sub>O<sub>2</sub> detection and for biosensors, *Talanta* 55 (2001) 605–611.
- [36] J.P. Coleman, A.T. Lynch, P. Madhukar, J.H. Wagenknecht, Printed, flexible electrochromic displays using interdigitated electrodes, *Solar Energy Mater. Solar Cells* 56 (1999) 395–418.
- [37] M.A. Pellitero, A. Colina, R. Villa, F.J. del Campo, Antimony tin oxide (ATO) screen-printed electrodes and their application to spectroelectrochemistry, *Electrochem. Commun.* 93 (2018) 123–127.
- [38] G. Ruiz-Vega, M. Kitsara, M.A. Pellitero, E. Baldrich, F.J. del Campo, Electrochemical lateral flow devices: towards rapid immunomagnetic assays, *ChemElectroChem* 4 (2017) 880–889.
- [39] A. Abellan-Lobregat, I. Jeerapan, A. Bandodkar, L. Vidal, A. Canals, J. Wang, et al., A stretchable and screen-printed electrochemical sensor for glucose determination in human perspiration, *Biosens. Bioelectron.* 91 (2017) 885–891.
- [40] G.L. Long, J.D. Winefordner, Limit of detection. A closer look at the IUPAC definition, *Anal. Chem.* 55 (1983) 712A–724A.
- [41] J.P. Coleman, A.T. Lynch, P. Madhukar, J.H. Wagenknecht, Antimony-doped tin oxide powders: electrochromic materials for printed displays, *Solar Energy Mater. Solar Cells* 56 (1999) 375–394.
- [42] R. Schiller, G. Battistig, J. Rabani, Reversible electrochemical coloration of indium tin oxide (ITO) in aqueous solutions, *Radiat. Phys. Chem.* 72 (2005) 217–223.
- [43] F. Ricci, A. Amine, G. Palleschi, D. Moscone, Prussian blue based screen printed biosensors with improved characteristics of long-term lifetime and pH stability, *Biosens. Bioelectron.* 18 (2003) 165–174.
- [44] N.B. Li, J.H. Park, K. Park, S.J. Kwon, H. Shin, J. Kwak, Characterization and electrocatalytic properties of Prussian Blue electrochemically deposited on nano-Au/PAMAM dendrimer-modified gold electrode, *Biosens. Bioelectron.* 23 (2008) 1519–1526.
- [45] E. Laviron, General expression of the linear potential sweep voltammogram in the case of diffusionless electrochemical systems, *J. Electroanal. Chem.* 101 (1979) 19–28.
- [46] H. Liu, R.M. Crooks, Paper-based electrochemical sensing platform with integral battery and electrochromic read-out, *Anal. Chem.* 84 (2012) 2528–2532.
- [47] H.A. Khorami, J.F. Botero-Cadavid, P. Wild, N. Djilali, Spectroscopic detection of Hydrogen peroxide with an optical fiber probe using chemically deposited Prussian Blue, *Electrochim. Acta* 115 (2014) 416–424.
- [48] A.P.F. Turner, I. Karube, G.S. Wilson, *Biosensors: Fundamentals and Applications*, 1st ed., Oxford University Press, New York, 1987.
- [49] M.A. Deshmukh, M. Gicevicius, A. Ramanaviciene, M.D. Shirsat, R. Viter, A. Ramanavicius, Hybrid electrochemical/electrochromic Cu(II) ion sensor prototype based on PANI/ITO-electrode, *Sens. Actuators B: Chem.* 248 (2017) 527–535.
- [50] R. Celiesiute, A. Ramanaviciene, M. Gicevicius, A. Ramanavicius, Electrochromic sensors based on conducting polymers, metal oxides, and coordination complexes, *Crit. Rev. Anal. Chem.* 4 (2018) 1–14.